AIP | Applied Physics Letters

# In situ atomic layer deposition half cycle study of Al2O3 growth on AlGaN

Barry Brennan, Xiaoye Qin, Hong Dong, Jiyoung Kim, and Robert M. Wallace

Citation: Appl. Phys. Lett. **101**, 211604 (2012); doi: 10.1063/1.4767520
View online: http://dx.doi.org/10.1063/1.4767520
View Table of Contents: http://apl.aip.org/resource/1/APPLAB/v101/i21
Published by the American Institute of Physics.

# In situ atomic layer deposition half cycle study of $Al_2O_3$ growth on AlGaN

Barry Brennan, Xiaoye Qin, Hong Dong, Jiyoung Kim, and Robert M. Wallace
*Department of Materials Science and Engineering, University of Texas at Dallas, Richardson, Texas 75080, USA*

(Received 10 August 2012; accepted 31 October 2012; published online 21 November 2012)

The atomic layer deposition (ALD) of $Al_2O_3$ on the native oxide and hydrofluoric acid treated $Al_{0.25}Ga_{0.75}N$ surface was studied using *in situ* X-ray photoelectron spectroscopy (XPS), after each individual "half cycle" of the ALD process. Initially, $Al_2O_3$, $Ga_2O_3$, and N-O states were detected on both surfaces at differing concentrations. During the course of the deposition process, the N-O bonds are seen to decrease to within XPS detection limits, as well as a small decrease in the $Ga_2O_3$ concentration. The $Al_2O_3$ growth rate initially is seen to be very low, indication of low reactivity between the trimethyl-aluminum molecule and the AlGaN surface. © *2012 American Institute of Physics*. [http://dx.doi.org/10.1063/1.4767520]

Due to the large bandgap and relatively high mobility of III-V nitride based materials, they are of significant interest in the fabrication of high electron mobility transistors (HEMTs) and other high power, high frequency, and high temperature devices.[1,2] However, these are known to experience significant surface related effects, such as large leakage currents[3] and frequency dependent current collapse.[4] One of the proposed methods to improve these devices is through the fabrication of metal-oxide-semiconductor HEMTs or hetero-field-effect-transistors (MOS-HEMTs or MOS-HFETs) by incorporating a high-k oxide layer between the semiconductor and the gate metal.[5,6] This would have the effect of significantly reducing leakage current, potentially improving mobility by preventing degradation of the semiconductor surface, and through passivation of the surface preventing current collapse by suppression of electron trapping at surface states, thereby providing increased reliability of MOS-HEMT based devices.[7,8] In terms of high-k deposition on these surfaces, atomic layer deposition (ALD) provides the most likely candidate for advanced device fabrication, due to the potential for high sample through put, controlled growth rates, and high aspect ratio conformal growth.

A number of studies have looked at the effect of different wet chemical treatments at removing native oxides and surface contamination from III-V nitride surfaces.[9,10] Hydrofluoric acid (HF) etching of GaN surfaces has previously been shown to produce one of the lowest oxide concentrations when compared to various other wet chemical treatments,[11] with only HCl seen to produce a marginally more oxide free surface.[12] Previous studies looking at $SiN_x/Al_2O_3$/AlGaN/GaN heterostructures showed low $D_{it}$ levels at the oxide/semiconductor interface,[13] and using a high-k $LaAlO_3$/$SiO_2$ bi-layers also on AlGaN/GaN structures, high drive currents, low threshold voltages, and high mobility were achieved with a capacitance extracted thickness for the high-k of 3 nm.[14] Hori *et al.* also report a reduction in interface state density on ALD $Al_2O_3$/AlGaN/GaN devices by employing a $N_2O$ radical treatment prior to ALD.[15] However, very little is reported about the chemical interactions that take place between deposited high-k materials and III-V nitride surfaces.[16] For this reason, this study looks at the effect of depositing $Al_2O_3$ by ALD on the native oxide and HF etched $Al_{0.25}Ga_{0.75}N$ surface, with X-ray photoelectron spectroscopy (XPS) carried out after successive "half cycles" of the ALD process,[17] to monitor the chemical changes at the semiconductor/high-k interface.

Undoped $Al_{0.25}Ga_{0.75}N$ (30 nm) samples, grown on a 1.2 $\mu$m GaN layer on a Si(111) substrate by metal organic chemical vapor deposition from DOWA Electronics Materials, were first solvent cleaned in acetone, methanol, and isopropanol for 1 min each. One sample was then etched in a 2% HF solution for 2 min, followed by a 2 min rinse in flowing deionized water and dried with nitrogen.[16] The sample was then immediately mounted to a sample plate along with an un-etched sample and introduced to an ultra-high vacuum (UHV) system. The UHV system, described in detail elsewhere,[18] consists of a number of vacuum chambers, each providing capabilities for various UHV deposition or characterization techniques, coupled together through a UHV transport tube maintained at a pressure of $< 1 \times 10^{-10}$ mbar, to allow for analysis after deposition without exposure to atmospheric conditions, which can introduce deleterious contamination and interfacial oxidation. In this study, ALD of $Al_2O_3$ was carried out on the AlGaN surfaces in a Picosun ALD reactor, at a substrate temperature of 300 °C. Trimethyl-aluminum (TMA) and $H_2O$ were used as the precursors for ALD, with a precursor pulse and purge time of 0.1 and 4 s, respectively. The base pressure of the ALD reactor was ~12 mbar, with ultra high purity $N_2$ used as the carrier and purging gas.

In order to monitor the $Al_2O_3$ growth on the AlGaN surfaces, XPS was carried out after loading the samples to UHV, upon exposing the samples to the ALD reactor at 300 °C under typical ALD conditions for 30 min, and after each individual "half cycle" pulse of the ALD process (such that the samples were first exposed to one pulse of TMA and scanned with XPS and then transferred back to the ALD reactor and exposed to one pulse of $H_2O$ and again scanned with XPS) up to two full cycles, as well as after 5, 10, and 20 full cycles (TMA + $H_2O$). The XPS was carried out using a monochromated Al k$\alpha$ ($h\nu = 1486.7$ eV) X-ray source, equipped with a 7 channel analyzer, using a pass energy of 15 eV, with all scans taken at 45° with respect to the sample normal. Spectra were taken of the Ga $2p_{3/2}$, Ga 3*d*, N 1*s*, Al 2*p*, O 1*s*, C 1*s*, F 1*s* core level regions as well as of the valence band edges. XPS peak deconvolution was carried out using AAnalyzer software[19] with a detailed peak fitting

 

procedure described elsewhere.[20] All peaks were referenced to the N 1*s* peak at 397.0 eV.

Atomic force microscope (AFM) images were obtained using an *ex situ* Veeco (Bruker) Multimode system in non-contact tapping mode, with root mean square (RMS) roughness measurements calculated using WSXM software,[21] and the final values determined by averaging RMS values taken from a number of regions on the surfaces. Images were taken of the initial surfaces (native oxide and HF etched) and after 20 cycles of $Al_2O_3$.

Based on the total oxygen concentration on the two samples upon introduction to UHV from the O 1*s* spectra (not shown), etching of the sample in HF reduced the concentration of oxygen by $>40\%$ relative to that seen on the native oxide sample. In order to determine where these changes to the substrate-oxide bonding were taking place, it was necessary to look at Ga, N, and Al core level spectra in more detail. The peak fitted Ga $2p_{3/2}$ and N 1*s* spectra after each individual stage in the deposition process are shown in Figure 1. The Ga 2*p* spectra in Figures 1(a) and 1(b) for the native oxide and HF etched samples, respectively, show evidence of two peaks; one at 1117.5 eV assigned to Ga bonded to AlN, and the other at 1118.2 eV, indicative of a Ga 3+ oxidation state, likely due to $Ga_2O_3$, consistent with previous reports.[22,23] There is no evidence of a Ga 1+ state, however, detection of this state is complicated due to the Ga-AlN peak having a similar binding energy to that of the $Ga_2O$ peak (1117.55 eV), as seen on GaAs and InGaAs samples.[24] Upon heating of the samples to 300 °C in the ALD reactor, there is a slight broadening of the Ga-AlN peak, such that the FWHM increases from 1.03 eV to 1.11 eV, which persists during subsequent ALD cycles. This could be evidence for formation of a low concentration of lower binding energy oxidation states or general disorder at the AlGaN surface.

The corresponding N 1*s* spectra in Figures 1(c) and 1(d) show the N-AlGa peak at 397.0 eV,[25] a N-O peak (possibly consisting of O, C, and H bonds) at ~400.5 eV,[26] as well as the Ga $L_2M_{45}M_{45}$ Auger feature (~392–398 eV). The Auger feature is fitted in such a way that the line-shape remains constant throughout and is consistent with line-shapes from previously reported spectra.[27] It should be pointed out that the commonly reported GaN-O bond at ~398 eV is likely to be a component of the Ga *LMM* Auger line, with an increase in this region usually appearing upon gallium oxidation. In order to show the changes in these spectra more clearly, the Ga 2*p* and N 1*s* core level spectra from the initial surfaces, after 300 °C anneal and after the first TMA pulse, are shown in Figure 2. Upon the first pulse of TMA, it is difficult to detect any obvious change in the Ga 2*p* spectra, however, from the ratio of the Ga 3+ peak area to that of the bulk peak, plotted in Figure 2(e), we find that there is a slight decrease in the concentration of Ga-O present on the surface as a result of interaction with TMA molecule. This is consistent with the "clean up" effect seen on other III-V semiconductors;[28] however, the extent of this interaction is much less on these surfaces, suggesting that there is a stronger bond between the Ga 3+ state and the AlGaN surface than with other materials. This inherent stability is also reflected in the oxide ratios when comparing the native oxide and HF etched surfaces, with the oxide ratio initially seen to be greater on the HF etched surface. Also, in a previous study by Sivasubramani *et al.*, which compared exposure of a GaN substrate to either a $H_2O$ or $O_3$ pulse,[16] and revealed that no oxidation was seen to take place upon exposure of the surface to $H_2O$. Upon exposure to the more aggressive $O_3$ oxidation, however, surface oxides were

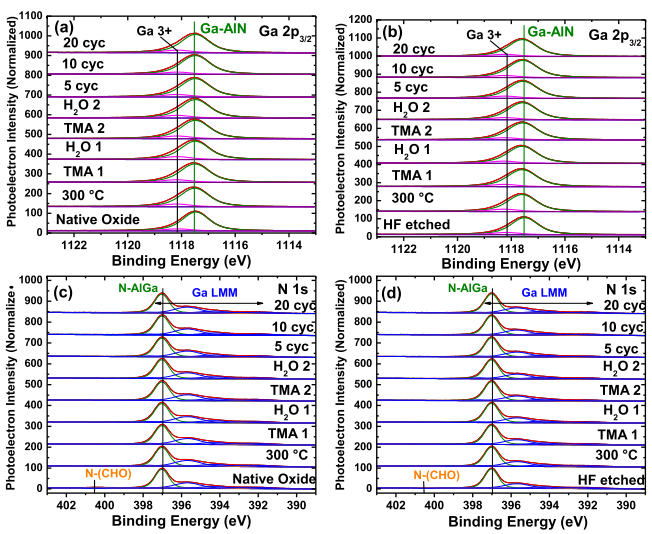


FIG. 1. XPS spectra of the Ga $2p_{3/2}$ (a) and (b) and N 1*s* (c) and (d) core levels from the native oxide (a) and (c) and HF etched (b) and (d) surfaces, from the initial surfaces, after annealing at 300 °C and each individual ALD half cycle deposition.

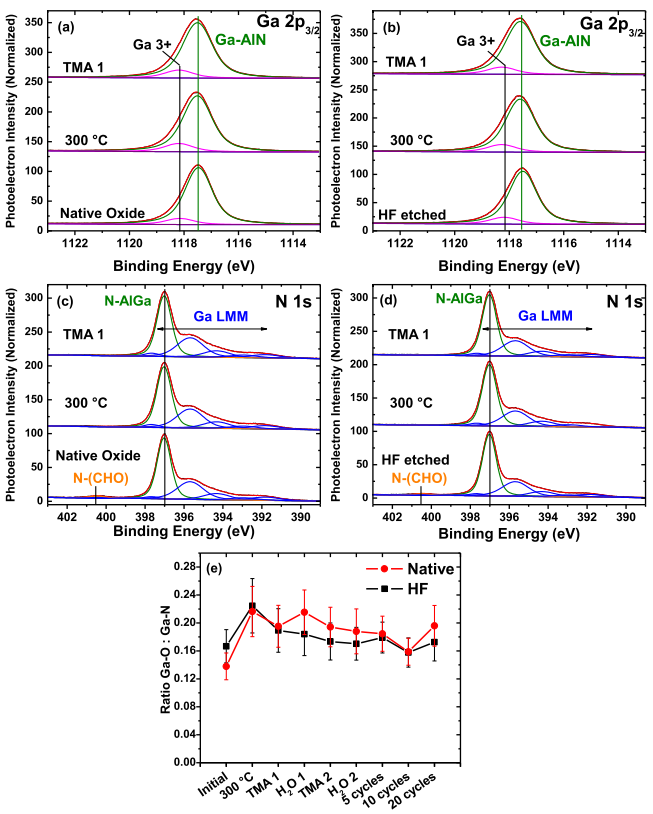


FIG. 2. XPS spectra of the Ga $2p_{3/2}$ (a) and (b) and N 1*s* (c) and (d) core levels from the native oxide (a) and (c) and HF etched (b) and (d) surfaces, from the initial surfaces, after annealing at 300 °C and after one pulse of TMA. (e) shows the ratio of gallium oxide to the bulk Ga-AlN peak from the Ga 2*p* spectra, indicating the changes in the gallium oxide present on the surface over the course of the deposition. Error bars were estimated to be ±9% based on the peak deconvolution and fitting procedures employed here.

seen to form which helped to promote subsequent $Al_2O_3$ nucleation. With successive cycles of TMA, we do detect an incremental decrease in the Ga-O:Ga-AlN ratio, again indicative of the "clean up" effect taking place, however, this trend is close to the associated error in the measurement. After 20 full cycles, the ratio is seen to increase again, with the highest level seen on the native oxide sample. From the N 1*s* spectra in Figures 2(c) and 2(d), we find that the N-O signal reduces to within detection limits after introduction to the ALD reactor at 300 °C. This is concurrent with an increase in gallium and aluminum oxide peaks, suggesting oxygen is transferring from the N-O bonding environments to form gallium and aluminum oxide. No further changes are detected in the N 1*s* spectra throughout the remainder of the deposition process.

Looking at the Al 2*p* spectra for the complete deposition process in Figures 3(a) and 3(b), and for the 300 °C annealed, after first "half cycle" of TMA and after 20 full cycles spectra in Figures 3(c) and 3(d), we detect the Al-GaN bulk peak at 73.5 eV, as well as trace amounts of $Al_2O_3$ at 74.4 eV. This is present on both the native oxide and HF etched surface initially and is observed to increase upon annealing, shown most clearly in the ratio of oxide to the bulk peaks in Figure 3(e). Subsequently, we detect an incremental increase in the $Al_2O_3$ peak after each successive TMA pulse, as indicated by the plot inset in Figure 3(e) showing the change in ratio during the initial stages of growth. However, this growth rate is much lower than typically expected. From XPS thickness calculations, based on the attenuation of the Ga 2*p* peak upon $Al_2O_3$ deposition, after 5 full cycles, we detect <0.1 nm of $Al_2O_3$ growth on both surfaces. With a further 5 full cycles, a similar growth rate is seen with ~0.2 nm of $Al_2O_3$ detected. However, after the next 10 cycles (20 total), the growth rate is observed to increase significantly, such that the final calculated thickness is 0.9 nm on the native oxide sample and 1.0 nm on the HF etched sample. This suggests that true ALD growth does not occur until a complete monolayer of oxide is formed on the surface and a number of ALD cycles are needed to instigate this growth. This variation in $Al_2O_3$ thickness on the two samples is further confirmed by the Al-O to Al-GaN ratio in Figure 3(e), with a greater final value observed for the HF etched sample, despite an initially higher ratio seen on the native oxide sample. With increasing $Al_2O_3$ thickness, the emergence of a higher binding energy peak in the Al 2*p* spectra, at ~75.3 eV, takes place, which suggests that there is some Al-OH incorporation into the films. A peak at 532.8 eV in the O 1*s* spectra (not shown) on both samples also suggests the presence of an –OH related state on both samples.

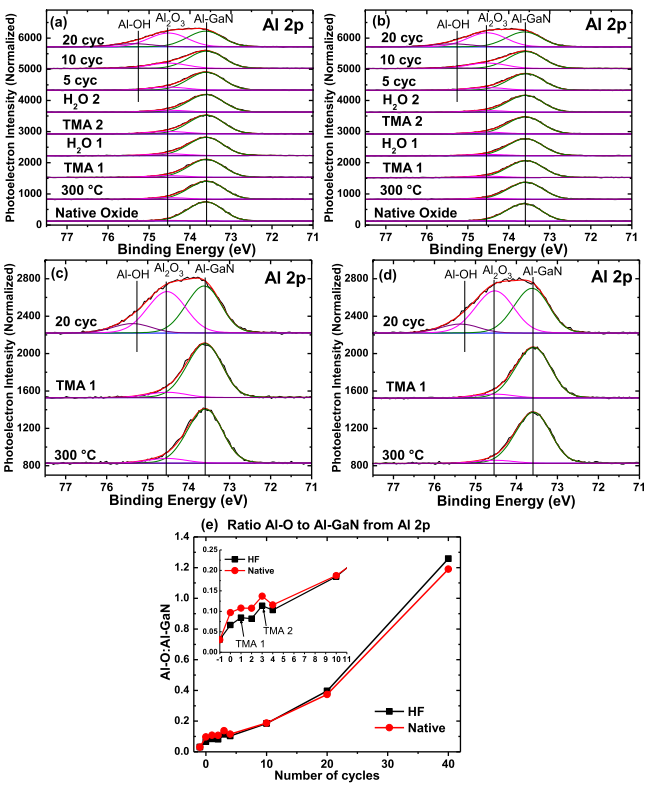


FIG. 3. Al 2*p* core level spectra from the native oxide (a) and (c) and HF etched (b) and (d) samples at various stages in the $Al_2O_3$ deposition process. Figure 3(e) shows the ratio of Al-O to Al-GaN from the same spectra indicating the change in $Al_2O_3$ growth rate with increasing number of ALD cycles. Inset shows the change in ratio during the initial ALD cycles.

A small concentration of fluorine was also detected on the HF etched sample, which was seen to decrease in concentration after annealing at 300 °C. However, upon subsequent ALD, no further changes in the level was detected. There was no evidence of any Ga or Al-F bonding in the Ga 2*p* or Al 2*p* spectra, where these bonds would be expected to form at higher binding energies than the oxide states due to the increased electronegativity of F relative to O, suggesting the F may at least initially be physisorbed to the surface. It is not clear what impact the presence of F at the interface between the AlGaN and the $Al_2O_3$ layer would have in terms of device performance. Further, there was no evidence of increased carbon concentration levels on the surfaces as a result of ALD, suggesting that there is no decomposition of the TMA molecule, other than that during ALD growth to form $Al_2O_3$.

From the valence band spectra (not shown), the valence band positions for the native oxide and HF etched samples were 2.09 and 2.17 ( ± 0.1) eV from the Fermi level, respectively, consistent with previous reports,[29] with no changes detected during the deposition process. This is consistent with the Fermi level being located at mid-gap for these undoped surfaces,[30] with no evidence of upwards band bending taking place after HF treatment, and would be indicative of a clean surface. This suggests that residual carbon or oxides left on the surface may still pose a problem and further processing, for example, high temperature or ammonia annealing,[31] is needed to generate a contamination free AlGaN surface prior to oxide deposition to prevent Fermi level pinning.

To comment further on the carbon present on the surface of both samples, the level of carbon detected, which is on the order of a monolayer in concentration, is not seen to increase over the course of the experiment, suggesting there is no significant incorporation of carbon into the $Al_2O_3$ film as a result of the ALD process. During the ALD half cycles, there is evidence of C-H (likely $AlCH_3$) and C-OH boding detected in the XPS spectra at various stages. Particularly on the HF etched sample, we see an increase in C-H bonding and a decrease in C-OH after TMA pulses, with the process reversed during the $H_2O$ pulses, consistent with a typical ALD process,[32] where a $CH_4$ molecule is removed upon interaction with the oxygen precursor, again, with no change in the total amount of carbon present.

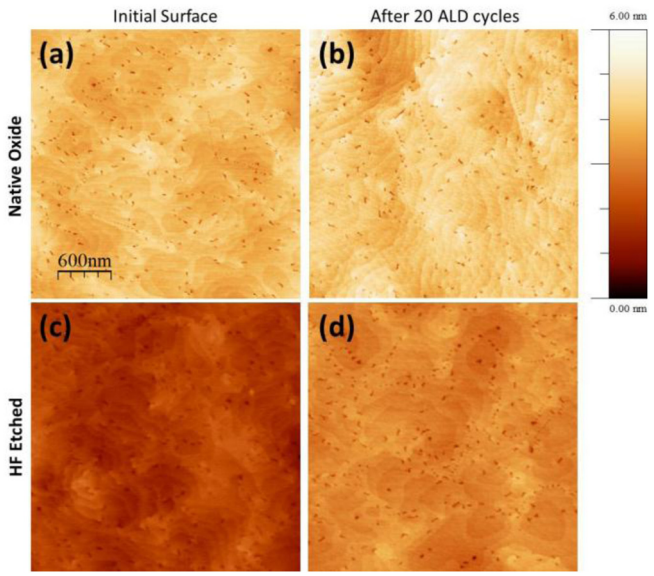


FIG. 4. AFM images ($3\,\mu m \times 3\,\mu m$) of the native oxide (a) and (b) and HF etched samples (c) and (d) from the initial surfaces and after 20 cycles of ALD. The contrasts have been adjusted so that all images have the same height scale.

In order to investigate whether there was any changes in the surface roughness as a result of the HF etch, AFM images were taken from the AlGaN samples before and after deposition. AFM images ($3\,\mu m \times 3\,\mu m$) taken from at least four different locations on the two samples, before and after 20 cycles of TMA, are shown in Figure 4, with clear evidence of the characteristic monolayer steps of the (Al)GaN surface seen,[33] even after deposition, indicating the conformal growth of the ALD $Al_2O_3$ despite the initial slow nucleation rate on the surface. The RMS roughness of the native oxide surface was calculated to be $0.30 \pm 0.05$ nm, increasing to $0.39 \pm 0.05$ nm after deposition. With HF etching, the RMS roughness is seen to decrease to $0.29 \pm 0.01$ nm, with only a slight increase, to $0.32 \pm 0.03$ nm, after ALD. This suggests that HF etching produces a more uniform surface, which may help to promote $Al_2O_3$ nucleation as evidenced by the increased final $Al_2O_3$ thickness on this surface. Reduced surface roughness is also likely to lead to improved carrier mobility by reducing the effect of surface scattering.[34] The appearance of dark regions is attributed to pits in the substrate that originate from the epitaxial process, and are widely reported in the literature (e.g., Ref. 33).

In conclusion, the initial stages of $Al_2O_3$ growth on the native oxide and HF treated AlGaN surface were investigated by XPS. Results suggest that the AlGaN surface is chemically very stable and that a number (>10) of ALD cycles are needed to initially nucleate the surface with $Al_2O_3$ before ALD growth is seen to take place. There is evidence of the ALD "clean up" effect taking place, with a decrease in the concentration of gallium oxide states seen upon interaction with the TMA molecule; however, this is not sufficient to fully remove the native oxides from the $Al_2O_3$/AlGaN interface. AFM measurements show a reduced surface roughness on the HF etched surface, with conformal ALD growth seen on both surfaces.

The authors would like to thank Professor Chris Hinkle, Dr. Stephen McDonnell, and Professor Albert Chin for their helpful discussions. This work was supported by the Asian Office of Aerospace Research and Development (AOARD) through the Air Force Office of Scientific Research (AFOSR) under Grant No. FA2386-11-1-4077, and the National Science Foundation under ECCS Award No. 0925844.

[1]S. J. Pearton and F. Ren, Adv. Mater. **12**, 1571 (2000).
[2]S. Strite and H. Morkoc, J. Vac. Sci. Technol. B **10**, 1237 (1992).
[3]J. W. Chung, J. C. Roberts, E. L. Piner, and T. Palacios, IEEE Electron Device Lett. **29**, 1196 (2008).
[4]B. M. Green, K. K. Chu, E. M. Chumbes, J. A. Smart, J. M. Shealy, and L. F. Eastman, IEEE Electron Device Lett. **21**, 268 (2000).
[5]A. L. Corrion, K. Shinohara, D. Regan, I. Milosavljevic, P. Hashimoto, P. J. Willadsen, A. Schmitz, S. J. Kim, C. M. Butler, D. Brown, S. D. Burnham, and M. Micovic, IEEE Electron Device Lett. **32**, 1062 (2011).
[6]T. Huang, X. Zhu, K. M. Wong, and K. M. Lau, IEEE Electron Device Lett. **33**, 212 (2012).
[7]T. Mizutani, Y. Ohno, M. Akita, S. Kishimoto, and K. Maezawa, IEEE Trans. Electron Devices **50**, 2015 (2003).
[8]Y. Ohno, T. Nakao, S. Kishimoto, K. Maezawa, and T. Mizutani, Appl. Phys. Lett. **84**, 2184 (2004).
[9]M. Dialea, F. D. Aureta, N. G. van der Berga, R. Q. Odendaala, and W. D. Roos, Appl. Surf. Sci. **246**, 279 (2005).
[10]H. Ishikawa, S. Kobayashi, Y. Koide, S. Yamasaki, S. Nagai, J. Umezaki, M. Koike, and M. Murakami, J. Appl. Phys. **81**, 1315 (1997).
[11]S. W. King, J. P. Barnak, M. D. Bremser, K. M. Tracy, C. Ronning, R. F. Davis, and R. J. Nemanich, J. Appl. Phys. **84**, 5248 (1998).
[12]R. Sohal, P. Dudekb, and O. Hilt, Appl. Surf. Sci. **256**, 2210 (2010).
[13]M. Miczek, C. Mizue, T. Hashizume, and B. Adamowicz, J. Appl. Phys. **103**, 104510 (2008).
[14]C. Y. Tsai, T. L. Wu, and A. Chin, IEEE Electron Device Lett. **33**, 35 (2012).
[15]Y. Hori, C. Mizue, and T. Hashizume, Phys. Status Solidi C **9**, 1356 (2012).
[16]P. Sivasubramani, T. J. Park, B. E. Coss, A. Lucero, J. Huang, B. Brennan, Y. Cao, D. Jena, H. Xing, R. M. Wallace, and J. Kim, Phys. Status Solidi (RRL) **6**, 22 (2012).
[17]M. Milojevic, C. L. Hinkle, F. S. Aguirre-Tostado, H. C. Kim, E. M. Vogel, J. Kim, and R. M. Wallace, Appl. Phys. Lett. **93**, 252905 (2008).
[18]R. M. Wallace, ECS Trans. **16**, 255 (2008).
[19]A. Herrera-Gomez, P. Pianetta, D. Marshall, E. Nelson, and W. E. Spicer, Phys. Rev. B **61**, 12988 (2000).
[20]B. Brennan and G. Hughes, J. Appl. Phys. **108**, 053516 (2010).
[21]I. Horcas, R. Fernández, J. M. Gómez-Rodríguez, J. Colchero, J. Gómez-Herrero, and A. M. Baro, Rev. Sci. Instrum. **78**, 013705 (2007).
[22]C. L. Hinkle, M. Milojevic, B. Brennan, A. M. Sonnet, F. S. Aguirre-Tostado, G. J. Hughes, E. M. Vogel, and R. M. Wallace, Appl. Phys. Lett. **94**, 162101 (2009).
[23]C. L. Hinkle, A. M. Sonnet, E. M. Vogel, S. McDonnell, G. J. Hughes, M. Milojevic, B. Lee, F. S. Aguirre-Tostado, K. J. Choi, H. C. Kim, J. Kim, and R. M. Wallace, Appl. Phys. Lett. **92**, 071901 (2008).
[24]C. L. Hinkle, E. M. Vogel, P. D. Ye, and R. M. Wallace, Curr. Opin. Solid State Mater. Sci. **15**, 188 (2011).
[25]F. González-Posada, J. A. Bardwell, S. Moisa, S. Haffouz, H. Tang, A. F. Braña, and E. Muñoz, Appl. Surf. Sci. **253**, 6185 (2007).
[26]J. F. Moulder, W. F. Stickle, P. E. Sobol, and K. D. Bomben, *Handbook of X-Ray Photoelectron Spectroscopy* (Physical Electronics Division, Perkin-Elmer Corporation, 1992).
[27]E. Antonides, E. C. Janse, and G. A. Sawatzky, Phys. Rev. B **15**, 1669 (1977).
[28]P. D. Ye, G. D. Wilk, B. Yang, J. Kwo, S. N. G. Chu, S. Nakahara, H. -J. L. Gossmann, J. P. Mannaerts, M. Hong, K. K. Ng, and J. Bude, Appl. Phys. Lett. **83**, 180 (2003).
[29]M. Higashiwaki, S. Chowdhury, B. L. Swenson, and U. K. Mishra, Appl. Phys. Lett. **97**, 222104 (2010).
[30]R. R. Pelá, C. Caetano, M. Marques, L. G. Ferreira, J. Furthmüller, and L. K. Teles, Appl. Phys. Lett. **98**, 151907 (2011).
[31]K. M. Tracy, W. J. Mecouch, R. F. Davis, and R. J. Nemanich, J. Appl. Phys. **94**, 3163 (2003).
[32]R. L. Puurunen, J. Appl. Phys. **97**, 121301 (2005).
[33]T. Hashizume, S. Ootomo, S. Oyama, M. Konishi, and H. Hasegawa, J. Vac. Sci. Technol. B **19**, 1675 (2001).
[34]B. Liu, Y. W. Lu, G. R. Jin, Y. Zhao, X. L. Wang, Q. S. Zhu, and Z. G. Wang, Appl. Phys. Lett. **97**, 262111 (2010).